Fabrication of glass-coated electrodes with nano and micrometer size by means of dissolution with HF

Fabrication of glass-coated electrodes with nano and micrometer size by means of dissolution with HF

Kochi Aoki*, Chaofu Zhang, Jingyuan Chen, Toyohiko Nishiumi

Department of Applied Physics, University of Fukui,

3-9-1 Bunkyo, Fukui-shi, 910 8507 Japan

Abstract

Platinum nano-electrodes were fabricated at the success rate 76 % by the six processes; (i) etching a Pt wire in ethanol-water mixture, (ii) sealing it with a glass sheath, (iii) grinding roughly the glass tip, (iv) polishing the tip while monitoring the capacitive ac-current flowing through the glass thin film on the Pt, (v) dissolving the glass film in HF solution until a part of Pt was exposed, and (vi) heating the tip at 85^{o}C for stabilization. A key of the process was to make a thin glass film on the Pt tip (iv) and to expose the Pt surface chemically by (v). 50 electrodes thus fabricated had diameters ranging from 1 nm to 5μm, estimated from the steady-state current of diffusion-controlled current of ferrocene in acetonitrile and ferrocenyl derivative in aqueous solution. They exhibited reproducible and stable voltammograms without hysteresis, withstanding 6 hours' continuous use and 15 hours' iterative processes of heat and voltammetry. Not only the halfwave potentials but also slopes of the log-plots were independent of radii of the electrodes. No kinetic effect was revealed in the steady-state voltammograms.

key-words: ultra-microelectrodes; steady-state voltammograms; Nernst plot; glass thin film; hydrofluoric acid

* corresponding author: kaoki@u-fukui.ac.jp (K. Aoki)

1. Introduction

An advantage of the voltammetric behavior at a microelectrode is to exhibit a steady-state current-voltage curve [1-3]. It is due to the existence of a mathematical solution for the 3D-diffusional Laplace equation [4]. The diffusion-controlled limiting current for the one-electron exchange reaction at the disk electrode a in radius is simply expressed by

$$I_L = 4Fc^*Da \qquad (1)$$

where c^* is the concentration of redox species, and D is its diffusion coefficient. The average current density, $j_L = (4/\pi)Fc^*D/a$, is enhanced with a decrease in the electrode diameter. On the other hand, the density at a large electrode is enhanced with an increase in scan rates, v, by cyclic voltammetry. When the expression for the current density is set equal to the equation of the peak current of linear sweep voltammetry ($j_p = 0.446Fc^*(DvF/RT)^{1/2}$), the scan rate can be expressed in terms of $v = 8.15RTD/Fa^2$. Typical values of v for a = 10 μm, 100 nm and 1 nm are, respectively, 2.1 V s^{-1}, 21 kV s^{-1}, 210 MV s^{-1} for $D = 10^{-5}$ cm^2 s^{-1} at 25°C. Therefore the steady-state voltammetry at nano-electrodes allows us to obtain such fast electron transfer kinetic data as not to be realized by the conventional fast scan voltammetry. Unfortunately, electron transfer rate constants of ferrocenyl compounds determined at nano-electrodes have varied from researcher to researchers [5-9]. They are sometimes consistent or sometimes inconsistent with those at fast scan CV [8-12], short pulse [13], ac impedance [10], and hydrodynamic voltammetry [14]. The wide variation of the rate constants may be ascribed to instability or an irreproducibility of microelectrodes, delay of a potentiostat at fast measurements, uncompensated resistance, and/or participation of capacitive currents.

A single nano-electrode has been fabricated by coating a thin metal wire with insulating films such as cathodic electrophoretic paint [15], by etching electrode tips by

flame [16,17] and electrochemical dissolution [18-20], by laser ablation [21,22], by microelectromechanical systems technologies [23], and by deposition of metals [24]. Although conventional techniques have already been established and surveyed [25,26], a number of inherent disadvantages still have been found, such as low success rate, poor reproducibility, fragility, temperature- and moisture-dependence, degradation of reversibility, and a short life. A long life has been attained by coating the electrode tips with glass [19,27-31] rather than with polymer films, because of low thermal expansion coefficient of glass, rigidity, low degree of swelling, and chemical proof. Unfortunately, it is not easy to control polishing a glass-sealed tip until predicted size of an active electrode is exposed. A strategy of the control is to monitor a degree of the exposure by dc current flowing through solution resistance between the electrode tip to a counter electrode [32]. A key is to stop the polishing immediately before the dc-current begins to flow. However, the Faradaic current by the high dc-voltage is caused by decomposition of water and salt to destruct the sealing and/or the active part, as we have often experienced damage of electrodes by applying such high voltage as salt or solvent is decomposed. Use of ac-voltage with small amplitude would not only keep off the damage but also leave behind a thin glass film on the electrode before exposing the metal. The thin glass film would be removed partially by chemical etching by hydrofluoric acid.

This report deals with fabrication of nano-electrodes by combining the six steps described in Abstract. The aim is to fabricate electrochemically endurable nano-electrodes at high success rate with minimal artifacts. Dissolution of glass by HF is a classical technique for fabrication of single electrodes [33-35], and has been applied to sharpening glass-tip arrays by meniscus etching [36]. However, it has not been used for fabrication of nano-electrodes yet, to our knowledge. Voltammetric properties at the nano-electrodes are examined for ferrocene (Fc) and its derivative.

2. Experimental

2.1. Fabrication

A platinum wire 0.03 mm in diameter was twisted around a tungsten wire 0.25 mm in diameter 10 times. The twisted part was hardened with electrically conducting resin. The etching conditions previously used were application of ac voltage, 5.0 V of 60 Hz for 10 min, in 6 M $NaNO_2$ solution to the Pt wire [37,38]. We found that the addition of more amount of ethanol made the wire more sharpened than in the aqueous solution. An increase in the amount of ethanol deceased solubility of salt. We used $CaCl_2$ for salt in the volume ratio 1/5 of ethanol/water. An example of the wire etched in 3 M $CaCl_2$ solution is shown in Fig. 1. A reason for forming a sharpened wire may be enhancement of natural convection by anodic dissolution due to low viscosity of ethanol. The etched tip was rinsed with the acid mixture (0.26 M acetic acid + 0.33 M nitric acid + 0.73 M phosphoric acid) for 1 min. The tip was inserted into a thermally pulled glass capillary 1.1 mm in inner diameter. The glass was melted with a flame of a spirit lamp to seal the Pt tip. The glass-sealed tip was ground on a rough emery paper until a glass film 0.1 mm thick was left behind on the Pt, by checking the tip with a video-microscope, VH-Z450 (Keyence, Osaka). SEM photograph was taken with JSM-6701F (JEOL, Tokyo).

The polishing-controlled apparatus is illustrated in Fig. 2, in which the Pt tip was to be polished on emery paper in 0.1 M KCl solution. The ac voltage with 0.1 V of 1 kHz was applied between the tip and the platinum coil for a counter electrode. The ac current detected with a potentiostat, NPGFZ-2501 (Nikko Keisoku), was amplified with a lock-in amplifier, MODEL 5210 (EG&G). The amplified output was recorded through a 12-bit AD-convertor, PCI-3521 (Interface), supported with a home-made software to be recorded against the time. The polishing was made by manual fashion while a current vs. time curve was being monitored. Polishing was stopped at a suitable value of the ac

current (described in Results). The polished tip was immersed in 0.98 M HF + 0.46 M NH_4OH + 0.79 M HNO_3 solution for a period from 2 to 10 min, rinsed with 30 w% KOH solution, rinsed with water, and then rinsed with the acid mixture (acetic acid + nitric acid + phosphoric acid). It was heated at 85^{o}C for 10 h in an oven in order to remove fluosilicate (described in Results section). The fabricated electrodes were kept in a dry box.

2.2. Chemicals

All the chemicals were of analytical grade. Aqueous ammonia, KOH, HNO_3 and $NaNO_2$ were purchased from Nakarai, and the others were from Wako. Ferrocenylmethyltrimethylammonium perchlorate (FcTMA) was synthesized and purified [38]. The experimenters treated hydrofluoric acid in a draft with a tail gas scrubber, wearing gas masks and latex gloves.

2.3. Voltammetry

Voltammetry was made in the three-electrode cell equipped with a working electrode, a Ag|AgCl reference electrode and a platinum coil counter electrode. The potentiostat was HECS 972 (Huso, Kawasaki), controlled with a homemade software. The electrode was rinsed with solvent before mounted in the cell. Voltammetry was carried out in deaerated solution in a Faraday cage.

3. Results and Discussion

The roughly ground glass-sealed Pt wire was mounted on the polishing apparatus in Fig. 2. Ac voltage (0.1 V amplitude at 1 kHz) was applied between the sealed Pt wire and the Pt coil, and the responding ac current was monitored with a help of the lock-in amplifier. The sealed Pt wire was polished by hand on a fine emery paper which was

immersed in 1 M KCl solution. As the polishing proceeded at the beginning of $t = 0$, the ac current, I_{ac}, (absolute values) was initially kept constant and then increased suddenly, as is shown in Fig. 3. The initial constant value may be caused by a delay or a capacitance of the potentiostat. The electrode at which polishing was ceased before the sudden increase did not show any voltammetric current in 0.5 M KCl + 0.5 mM FcTMA solution. The period before the sudden increase (43 s in Fig. 3) varied from electrodes to electrodes, depending on thickness of the glass film left on the sealed Pt tips. Thicker glass films took longer period, judging from views of the optical microscope. The sudden increase in I_{ac} (at $t = 43$ s in Fig. 3) suggests initiation of the exposure of an active part of the Pt to the solution.

It seems reasonable to consider that an active Pt surface is exposed just at the time of the sudden increase, as illustrated in Fig. 3(c). We ceased the polishing at a given exposure time, t_{xps}, after observing the sudden increase, and transferred the electrode to the FcTMA solution for voltammetry. The voltammograms were under the steady-state without hysteresis. From the limiting current of Eq.(1), we evaluated the radii with the help of the value of the diffusion coefficient of FcTMA, $D = 6.3\times10^{-6}$ cm^2 s^{-1}. The values of the diameter were plotted against the exposure period in Fig. 4 for 34 electrodes. Shorter exposure periods decreased the radii. Scattering in the plot was so large that the radii could not be controlled by the polishing period. The scattering was sensitive neither to fineness of emery paper, kinds of polishing pad with alumina powder, pressure of polishing, nor polishing speed, probably because artificial manipulation of the hand-polishing influences more strongly on the scattering than these factors. Polishing for periods less than 6 s scarcely exposed electroactive part (shown as marks X in Fig.4), as illustrated in Fig. 3(b). Our initial aim was to fabricate size-controlled electrodes with $2a < 1$ μm by adjusting t_{xps}, but has not been fulfilled in reproducibility.

A possible strategy of controlling radii of nano-electrodes is to dissolve the thin

glass film on the Pt tip slowly by chemical etching in HF solution. When the polishing was stopped within t_{xps} < 5 s, no active area was exposed (see Fig. 4 and Fig. 3(b)). The glass-sealed Pt was immersed into the HF solution for the period, t_{HF}, of less than 6 min, and then was rinsed with KOH solution and water successively. The rinsed tip was used for voltammetry in FcTMA solution in order to estimate its diameter. Electrodes treated by 1 min's dissolution were mostly electrochemically inactive. The dissolution for t_{HF} = 2 min provided a number of electrodes with $2a$ < 100 nm. Longer dissolution provided larger diameters, as is shown in Fig. 5. However, scattering of the radii was too large to be regarded as "a size-controlled process".

In order to examine reproducibility of the voltammograms, we iterated the following process composed of voltammetry of FcTMA solution, rinse of the electrode with water and keeping it in air for an hour. The limiting current enhanced gradually at each iterative process, implying expansion of the exposed area. The dissolution may be advanced even after removal of HF. When dissolution of glass with HF is terminated by alkali metal hydroxide, fluorosilicate has generated on the glass surface in gel form, which causes slow dissolution of glass [39]. In order to terminate the dissolution completely, we attempted to heat the electrodes at several temperatures in an oven for ten hours. We found that heating at 85^{o}C was able to stabilize the voltammograms.

The overall success rate of the fabrication was 76 %, which is a product of the success rate 80 % of the process till the polishing for t_{xps} and the rate 95 % of the heating. Since the key process of the exposure is due to the chemical dissolution of the glass, the fabrication includes little artifact manipulation. At this state, the electrode size has not been known. The accurate size has to be evaluated by voltammetric limiting currents, as described in the next section. However, it is desirable to predict at least the order of diameters, immediately after the fabrication. By comparing the accurate values by voltammetry with the combination of t_{xps} and t_{HF}, we found empirically that the order of the diameters could be estimated at the end of the fabrication so far as $2a$ > 1 μm. We

have examined this fabrication technique to gold wire successfully.

Figure 6 shows two examples of the voltammograms of (a) Fc in tetraethylammonium tetrafluoroborate ($TEABF_4$) included acetonitrile and (b) FcTMA in KCl aqueous solution. The glass-coating allowed us to carry out voltammetry both in aqueous solution and aprotic solution. Even if the electrode was transferred alternatively between the acetonitrile solution and the aqueous solution, every two voltammograms were overlapped. The voltammograms were not only sigmoid under the steady state without hysteresis but also reproducible at iterative scans. The background oxidation currents in Fig. 6 are due to insufficient non-zero adjustment of the potentiostat. Diameters of these electrodes evaluated from the limiting currents, the concentrations and the diffusion coefficients through Eq.(1) are $2a$ = (a) 4.7 nm at $D = 1.7\times10^{-5}$ cm^2 s^{-1} in acetonitrile and (b) 2.8 nm at $D = 6.3\times10^{-6}$ cm^2 s^{-1}.

Geometry of the most electrodes was uncertain because of the difficulty in identification of the electrode surface by SEM. However, we estimated the size from Eq. (1) on the assumption of disk-shape. The other available model geometry is a hemisphere a in radius, of which diffusion-controlled current is given by $(I_L)_{hs} = 2\pi Fc^*Da$. The radius evaluated from the current through this equation is smaller by $\pi/2$ ($\approx$ 1.5) times than the value obtained from Eq. (1). Since we are aiming at demonstrating a negligible effect of the electron transfer rate constant on the electrode size, the difference of the 1.5 times is within errors.

The stabilization of the electrodes was examined by multi-scan voltammetry for the continuous measurements and the intermittent voltammetry at each hour during which the electrode was dried and heated. Multi-scan voltammograms at v = 10 mV s^{-1} showed no distortion of the waveform or no potential shift for 6 h. Figure 7A shows variation of the limiting currents of FcTMA at iterative scans. The currents have no systematic time-variation, of which value is smaller than the standard deviation (0.20 pA). Thus, neither contamination of the electrode nor expansion of the active area

occurred. The conditions of the intermittent voltammetry included three-scan voltammetry → rinse → drying at 50°C for 15 min → being kept in air for 40 min or longer. All the voltammograms had no hysteresis. The limiting currents were plotted against the lapse of the process in Fig. 7B, showing no systematic variation for 16 h both in aqueous and acetonitrile solutions. The scattering in Fig. 7B is larger than that in Fig. 7A because the former involved the heating.

Available models of diffusion-controlled currents and electrode kinetics at microelectrodes are for a disk and a hemispherical electrode. In order to determine which model is suitable for the fabricated electrodes, we tried to obtain SEM images of the surface of microelectrodes, from which their geometry and diameter could be evaluated. After getting sufficient amounts voltammetric data at a give electrode, we cut the tip of the electrode by 8 mm, keeping the tungsten lead exposed to the other end. The tip was mounted up in a hole of stainless steel block so that the tungsten lead came in electrical contact with the block. Various SEM images were recorded by varying voltage, magnification, and tilt of the electrode tip. We found many white dots and black dots on the glass surface although there was only one exposed electrode. There were some dots of which diameters were close to the diameter evaluated from the voltammetry. A key is identification of the electrode surface. We attempted to identify an electrode more than 5 μm in diameter by the optical microscope. Photographs by the reflection optical microscope showed many white dots, one of which should be a true electrode because the incident light is reflected strongly on the Pt surface. On the hands, those by transmission optical microscope showed also many black dots, one of which should be a true electrode because the incident light should be blocked by the Pt. We overlapped the two photographs, and regarded dots with logical AND between the black and the white dots as a true electrode. However, there were more than one dots, of which coordinates on the photograph were recorded. The electrode was transferred to the SEM. All the portions at the recorded coordinates looked black dots with low

magnification and high accelerating voltage. As the voltage decreased, one of the black dots was found to be composed of two concentric circles, a large grey dot and a small black dot. Since size of the large one varied with magnification and the voltage, it should be a virtual image. The central small one was kept in size by change in the voltage, which should be a true electrode, as is shown in Fig. 8. We confirmed that there was only one dot on the tip surface that had the above properties. When curve fitting for a circle was applied to the photograph, the diameter was slightly smaller than the value obtained from the limiting current. The above technique was valid only for electrodes more than 2 μm in diameter because of the restriction of the performance of the optical microscope.

In order to demonstrate the quality of the steady-state voltammograms, we plotted values of $\log[I/(I_L - I)]$ against E in Fig. 9 for FcTMA and Fc. Both plots fell on each line for $0.1 < I/I_L < 10$. Values of the inverse slopes in Fig. 9 were 63 mV and 59 mV, respectively, for FcTMA at a = 99 nm and Fc at a = 2.4 nm. The other electrodes also showed linear log-plots, of which inverse slopes were fluctuated from 55 mV to 75 mV.

A feature of the steady-state voltammograms is the halfwave potential, $E_{1/2}$. It was read at each voltammogram within 1 mV hysteresis errors. The values were plotted in Fig. 10 against the logarithmic radii evaluated from the limiting currents for FcTMA (circles) and Fc (triangles), where some electrodes were used commonly to FcTMA and Fc. The halfwave potentials of both FcTMA and Fc were independent of the radii over the range of $a > 1$ nm, showing the average values, $E_{1/2}$(FcTMA) = 0.404 ± 0.025 V and $E_{1/2}$(Fc) = 0.056 ± 0.004 V, where the errors denote the standard deviations. The larger standard deviation for the aqueous solution may be associated with higher possibility of broadening voltammograms, or of including capacitive current. The average current density at the smallest electrode ($2a$ = 1.1 nm) was 2.3×10^3 A cm^{-2}, which corresponds to the scan rate, 450 M V s^{-1} at a large electrode, according to the discussion in Introduction. It is dangerous at present to discuss a reason why the high current density

exhibited no potential shift by electron transfer rates, because nano-materials often activate reaction rates.

4. Conclusions

Reproducible fabrication of nano-electrodes has been realized by the six steps:

(i) sharpening in 3 M $CaCl_2$ ethanol|water solution (1:5 ratio) by electrochemical etching

(ii) sealing the Pt wire in glass sheath

(iii) grinding the glass-sealed tip until the glass film became 0.1 mm thickness

(iv) polishing the tip while monitoring the ac current for $t_{xps} < 6$ s

(v) dissolution of glass film in HF for $t_{HF} \leq 4$ min

(vi) stabilization by heating at 85^{o}C for 10 h

Although the polishing period for $t_{xps} < 6$ s was predicted to be a predominant size-determining variable, it included artificial manipulation. Step (iv) generated such a glass thin film as to be dissolved slowly with HF. The actual exposure was realized by step (v). Although combination of steps (iv) and (v) failed to control diameters of the electrodes, electrodes with $2a < 1$ μm were able to be fabricated at success rate 76 %. Consequently, we could obtain a number of nano-electrodes.

Figure Captions

Figure 1. Photographs of Pt wires 0.03 mm in diameter, which were tapered in the etching solutions of (A) 3 M $CaCl_2$ ethanol-water (v/v 1/5) solution and (B) 6 M $NaNO_2$ aqueous solution.

Figure 2. Illustration of the apparatus for monitoring the ac current during polishing the glass-sealed Pt wires.

Figure 3. Time-variation of ac current (absolute values) during polishing the glass-sealed Pt wire of which images are illustrated in (a)-(c) when ac voltage of 0.1 V at 1 kHz was applied to the Pt wire in 0.1 M KCl solution.

Figure 4. Dependence of the radii evaluated from the limiting current of FcTMA oxidation through Eq.(1) on the exposure time, t_{xps}. Mark x means zero limiting current.

Figure 5. Variation of the diameters of the electrodes with the period, t_{HF}, during which the glass film of the glass-sealed Pt wire was dissolved in 0.98 M HF + 0.46 M NH_4OH + 0.79M HNO_3 solution. The arrow means the presence of unexposed Pt.

Figure 6. Voltammogram of (a) 5.34 mM Fc in 0.5 M $TEABF_4$ acetonitrile solution and (b) that of 2.11 mM FcTMA in 0.1 M KCl aqueous solution at v = 10 mV s^{-1}. Diameters of the electrodes calculated from the limiting currents are (a) 4.7 nm and (b) 2.8 nm.

Figure 7. Time-variations of the limiting currents of (circles) 2.11 mM FcTMA in 0.1 M KCl aqueous solution and (triangles) 5.34 mM in in 0.5 M $TEABF_4$ acetonitrile solution in the (A) multi-scan voltammetry and (B) intermittent voltammetry at v = 10 mV s^{-1}. The electrode diameters were (A) 25 nm and (B) 0.40 (circles) and 0.50 (triangles) μm from the averaged values of the limiting currents.

Figure 8. SEM photograph of the exposed Pt electrode from the glass insulator.

Figure 9. Log plots, $\log[I/(I_L - I)]$, vs. potentials of voltammograms for FcTMA (circles) at a = 99 nm and Fc (triangles) at a = 2.4 nm.

Figure 10. Dependence of the halfwave potential of FcTMA (circles on the right axis) and Fc (triangles on the left axis) on the logarithmic radii of the electrodes.

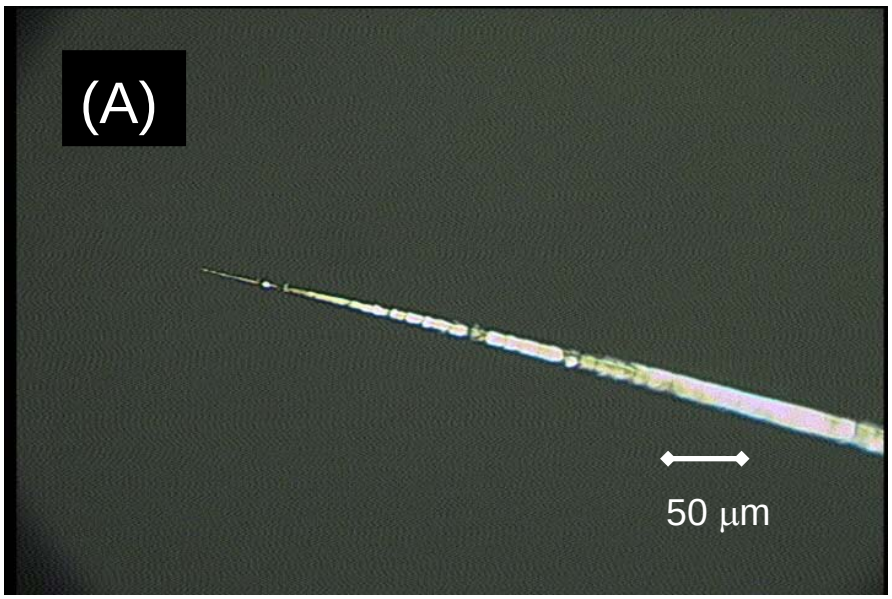

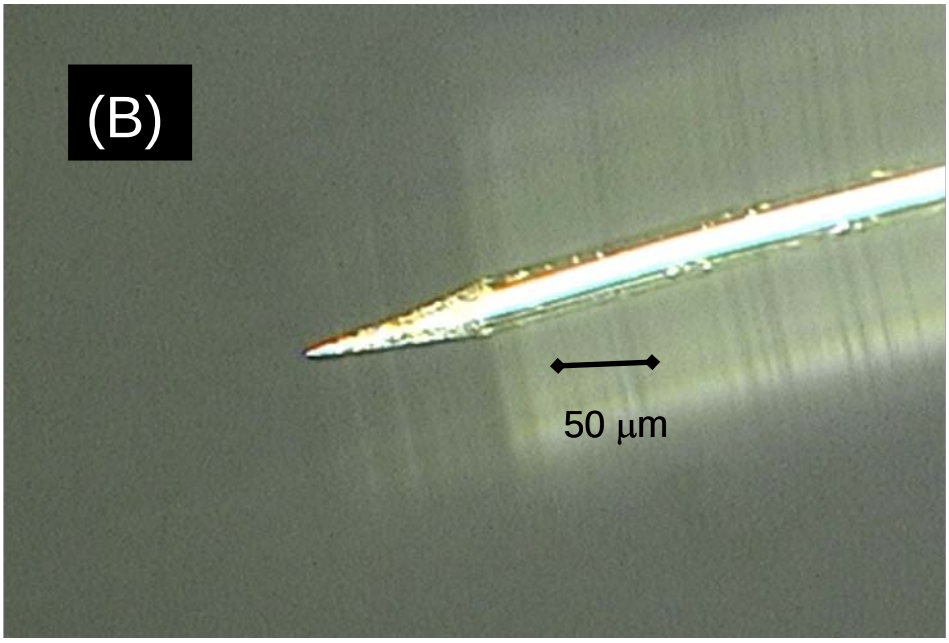

Figure 1

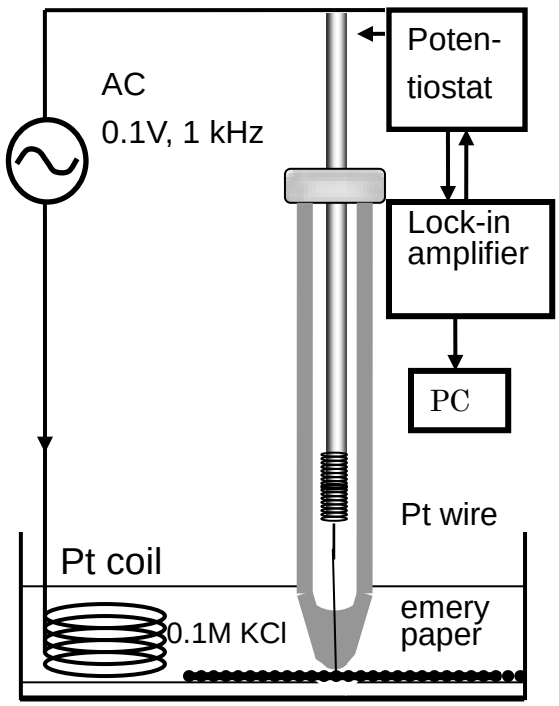

Figure 2

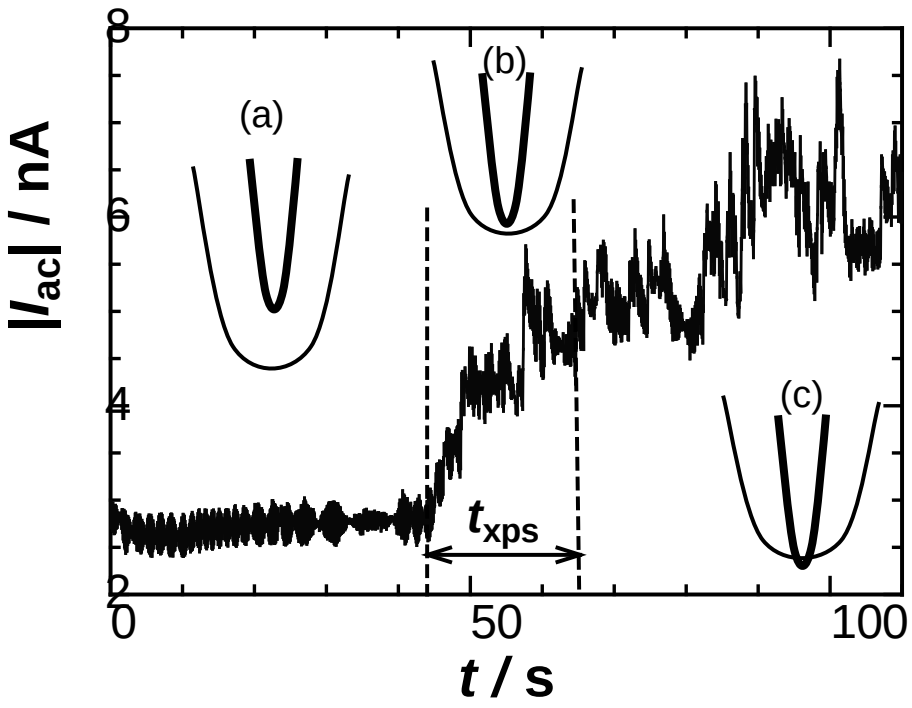

Figure 3

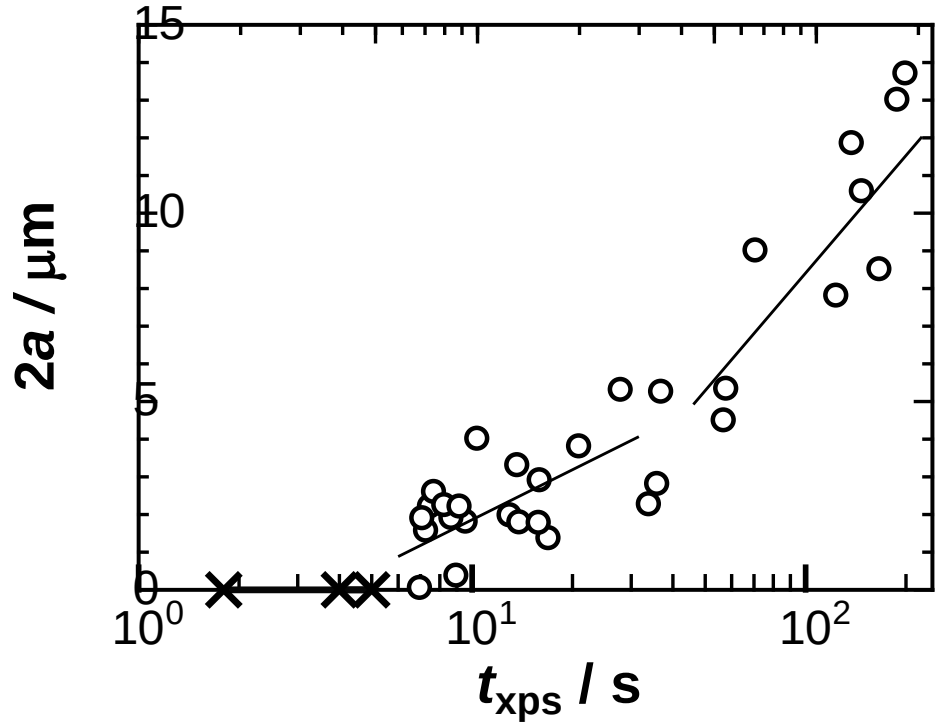

Figure 4

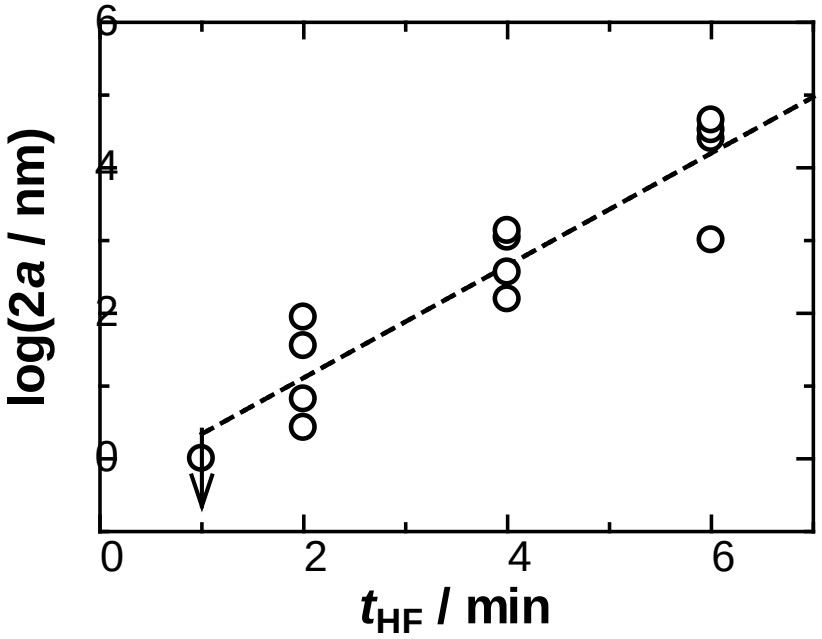

Figure 5

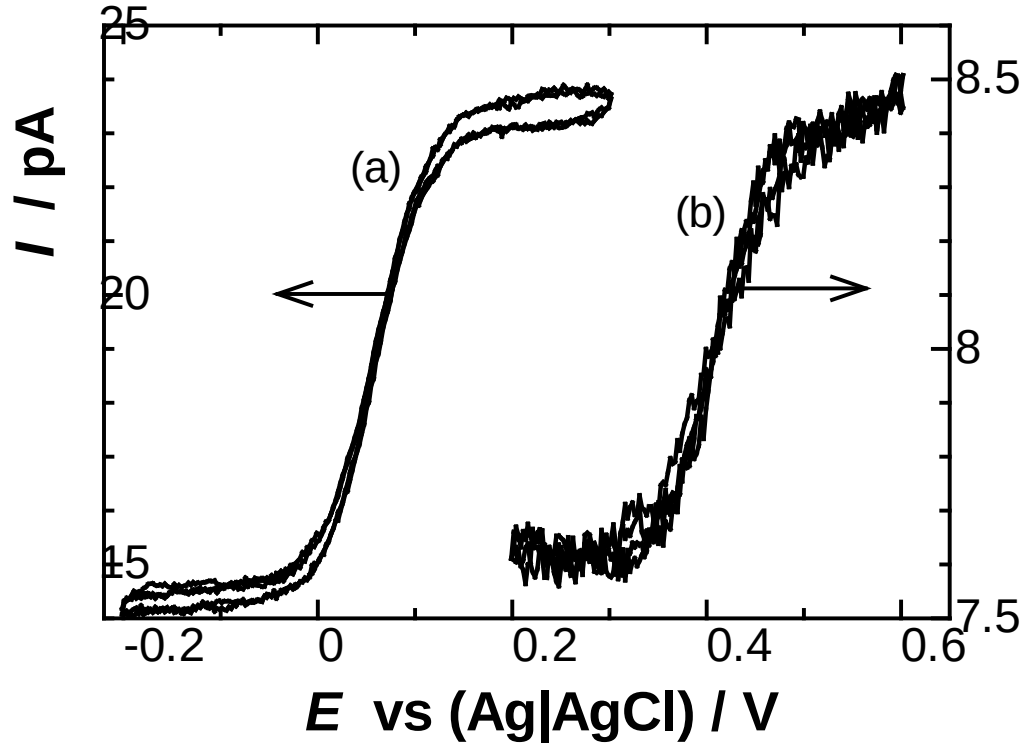

Figure 6.

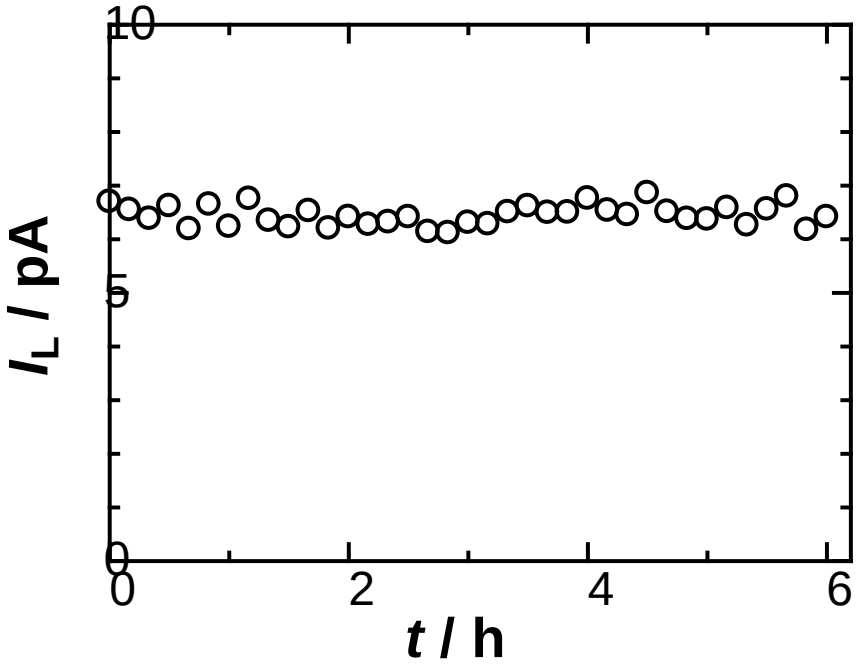

Figure 7A

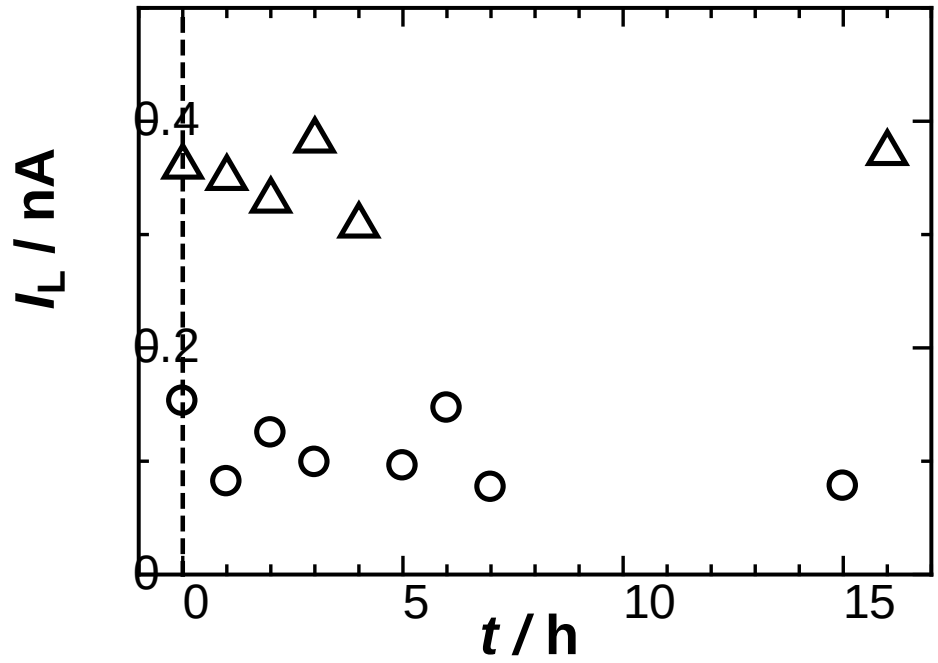

Figure 7B

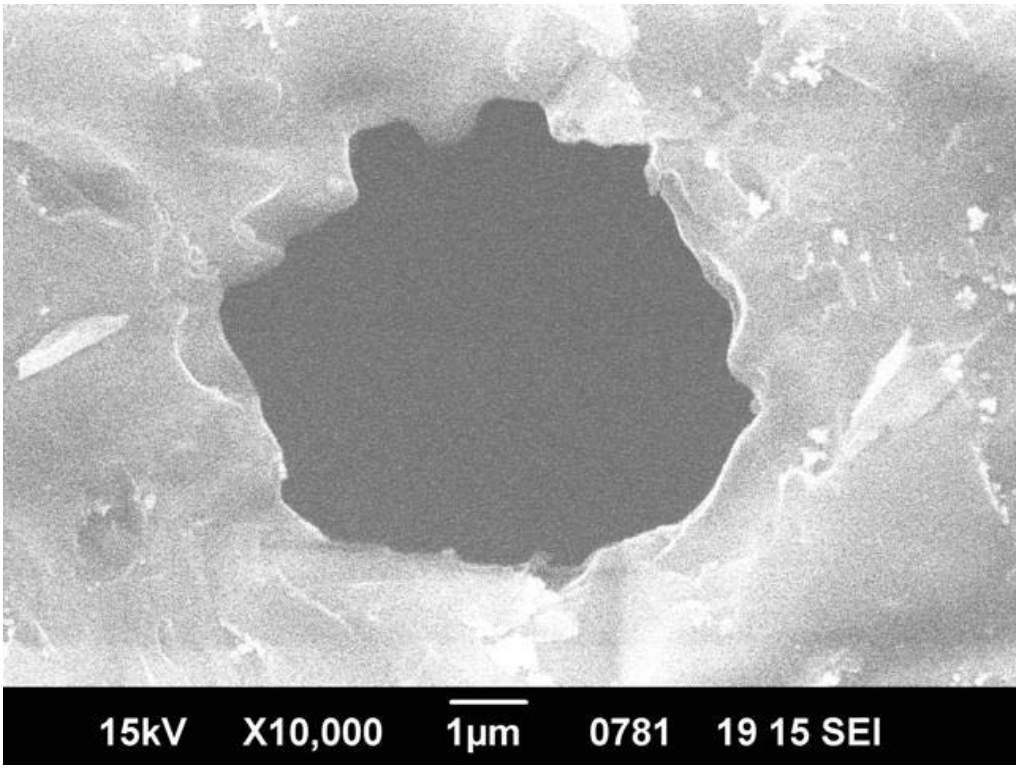

Figure 8

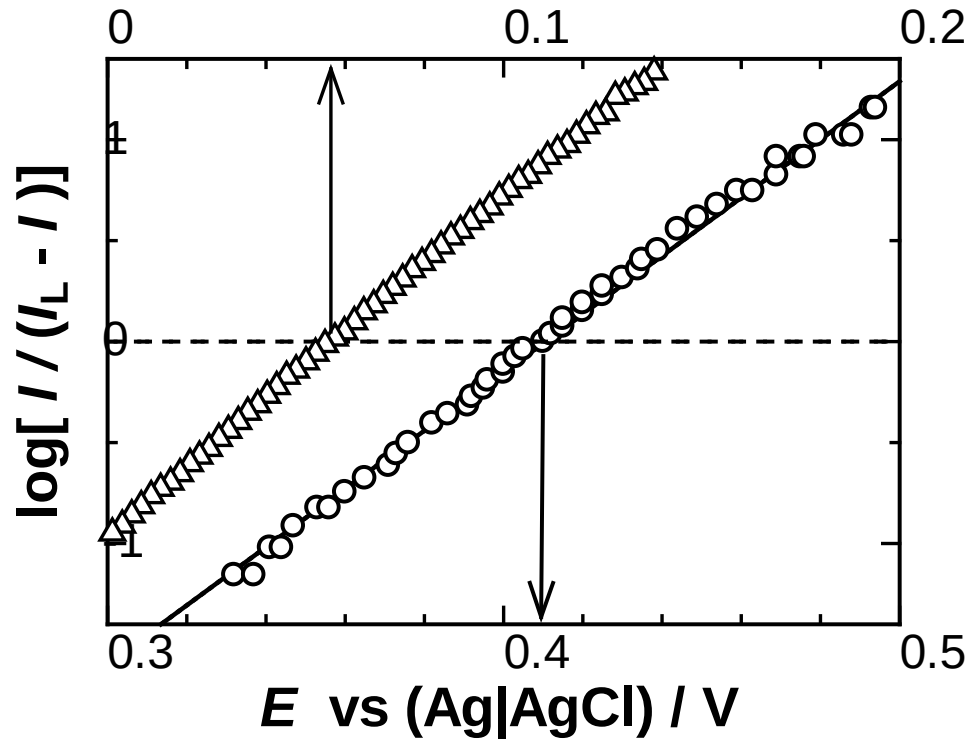

Figure 9

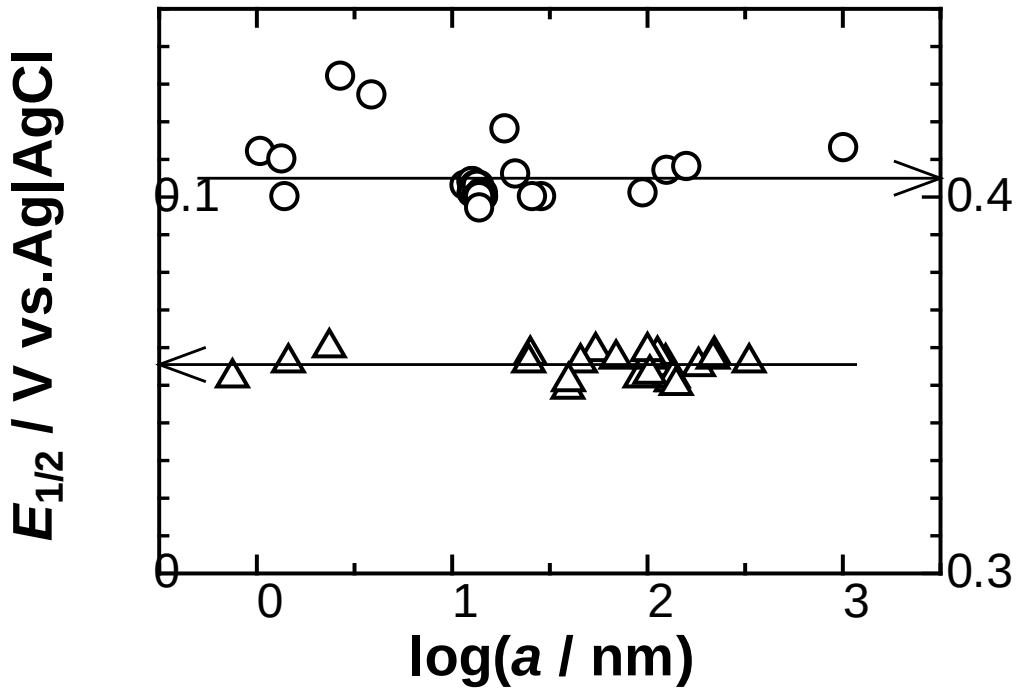

Figure 10

References

[1] A. J. Bard, L. R. Faulkner, Electrochemical Methods, 2nd Ed., John Wiley, New York, 2001, p. 176.

[2] K. Aoki, Electroanalysis 5 (1993) 627.

[3] J. Heinze, Angew. Chem. 32 (2003) 1268.

[4] D. J. Griffiths, Introduction to Electrodynamics, 2nd ed. Prentice Hall, New Jersey,1989, pp.1120-120.

[5] R. M. Penner, M. J. Heben, T. L. Longin, N. S. Lewis, Science 250 (1990) 1118.

[6] J. J. Watkins, J. Chen, H. S. White, H. D. Abruna, E. Maisonhaute, C. Amatore, Anal. Chem. 75 (2003) 3962.

[7] M. V. Mirkin, T. C. Richards, A. J. Bard, J. Phys. Chem., 97 (1993) 7672.

[8] W.R. Fawcett, M. Opallo, Angew. Chem. 106 (1994) 2239.

[9] A.M. Bond, T.L.E. Henderson, D.R. Mann, T.F. Mann, W.Thormann, C.G. Zoski, Anal. Chem. 60 (1988) 1878.

[10] A. S. Baranski, K. Winkler, W. R. Fawcett, J. Electroanal. Chem. 313 (1991) 367.

[11] D. O. Wipf, E. W. Kristensen, M. R. Deakin, R. M. Wightman, Anal. Chem. 60 (1988) 306.

[12] A. P. Abbott, C. L. Miaw, J. F. Rusling, J. Electroanal. Chem. 327 (1992) 31.

[13] Z. J. Karpinski, R. A. Osteryoung, J. Electroanal. Chem. 349 (1993) 285.

[14] A. D. Clegg, N. V. Rees, O. V. Klymenko, B. A. Coles, R. G. Compton, J. Electroanal. Chem. 580 (2005) 78.

[15] Y. Qiao, J. Chen, X. Guo, D. Cantrell, R. Ruoff, J. Troy, Nanotech. 16 (2005) 1598.

[16] T. G. Strein, E. W. Ewing, Anal. Chem. 64 (1992) 1368.

[17] T. Malinski, Z. Taha, Nature 358 (1992) 676.

[18] K. T. Kawagoe, J. A. Jankowski, R. M. Wightman, Anal. Chem. 63 (1991) 1589.

[19] A. Schuite, R. H. Chow, Anal. Chem. 70 (1998) 985.

[20] W.-H. Huang, D.-W. Pang, H. Tong, Z.-L. Wang, J.-K. Cheng, Anal. Chem. 73 (2001) 1048.

[21] Y. Liao, J. Xu, H. Sun, J. Song, X. Wanga, Y. Cheng, Appl. Surf. Sci. 254 (2008) 7018.

[22] S. Kumar, R. Kumar, A. K. Shukla, L. M. Bharadwaj, Mat. Let. 61 (2007) 3829.

[23] J. H. Lee, Y. Seo, T. S. Lim, P. L. Bishop, I. Papautsky, Environ. Sci. Technol. 41 (2007) 7857.

[24] A. Hermans, R. M. Wightman, Langmuir 22 (2006**)** 10348.

[25] C. G. Zoski, Electroanalysis 14 (2002) 1041.

[26] R. M. Wightman, Science 311 (2006) 1570.

[27] R. M. Penner, M. J. Heben, N. S. Lewis, Anal. Chem. 61 (1989) 1630.

[28] B. D. Pendley, H. D. Abruna, Anal. Chem. 62 (1990) 782.

[29] C. Lee, C. J. Miller, A. J. Bard, Anal. Chem. 63 (1991) 78.

[30] C. G. Zoski, B. Liu, A. J. Bard, Anal. Chem. 76 (2004) 3646.

[31] G. Wang, A. K. Bohaty, I. Zharov, H. S. White, J. Am. Chem. Soc. 128 (2006) 13553.

[32] B. Zhang, J.Galusha, P. G. Shiozawa, G. Wang, A. J. Bergren, R. M. Jones, R. J. White, E. N. Ervin, C. C. Cauley, H. S. White, Anal. Chem. 79 (2007) 4778.

[33] E. J. Neafsey, Brain Res. Bull. 6 (1981) 95.

[34] F. Wörgötter, U.T. Eysel, J. Neurosc. Meth. 25 (1988) 135.

[35] G. Shi, L. F. Garfias-Mesias, W. H. Smyrl, J. Electrochem. Soc. 145 (1998) 2011.

[36] J.-H. Lee, A. Jang, P. R. Bhadri, R. R. Myers, W. Timmons, F. R. Beyette Jr., P. L. Bishop, I. Papautsky, Sens. Actuators B 115 (2006) 220.

[37] J. Chen, K. Aoki, Electrochem. Commun. 4 (2002) 24.

[38] K. Aoki, J. Chen, H. Zhang, J. Electroanal. Chem. 610 (2007) 211.

[39] M. J. Krasinski, K. R. Krasinska, Z. Ulanowski, Crys. Res. Tech. 42 (2007) 1237.